Supporting Information

Nair et al. 10.1073/pnas.1712431115

SI Low-Frequency Power Modulations in Home Cage and Arena

In addition to the results reported in the main text, which focus entirely on modulations of gamma oscillations, we report here the effects in the low-frequency bands with particular focus on the delta band (1–5 Hz), theta band (6–10 Hz), and beta band (12–30 Hz). Fig. S1 shows examples of spectrograms recorded in the BF, ACC, and VC of a single rat, computed using the methods described in the main text.

In addition to the fluctuations in the gamma band, which are analyzed in the main text, prominent peaks are seen in the theta band in all three brain regions, and environmental context-dependent (i.e., arena vs. home cage) fluctuations are seen in the delta and beta bands. The theta peaks are particularly interesting, in that they exhibit selectivity opposite that observed in the gamma band. While gamma is enhanced in the home cage, theta is suppressed, so that in this example the theta peak virtually disappears in the home cage. Theta peaks and enhanced arena vs. home cage values are also present in the ACC and VC. Additional less pronounced features of the LFP power distributions are elevated delta and beta oscillations in home cage in the ACC and BF. Note that while delta activity is larger in the home cage than in the arena, these delta oscillations are not related to sleep, and indeed delta activity during sleep manifests as broad-band power increases from 1 to 20 Hz in the BF (see figure 2*A* in ref. 1).

To validate these observations across animals, we computed power in the different frequency bands for each brain region and compared values using t tests (Fig. S2). The analysis confirms that the effects observed in the single-animal example shown are significant at the group level. In the BF, in addition to the gamma enhancement in the home cage, beta and delta oscillations are also elevated, whereas theta power is strongly suppressed relative to values recorded in the arena. A similar pattern is observed in ACC, where gamma, beta, and delta power are enhanced in the home cage but theta power is not significantly different in the two environments. In the VC the strongest effect is related to enhanced theta power in the arena; the only other significant difference is in the high gamma band (above 60 Hz), where values are enhanced during locomotion, as discussed in the main text.

SI Distributions of Theta and Gamma Power Within Each State Are Unimodal

Here we aim to examine in more detail the dynamics of gamma and theta LFP power during each behavioral state. In Fig. S3, *Left*, gamma power is plotted against theta power for segments of 2-s duration with about 20 min of data shown during both arena-exploration and home-cage conditions. The histograms for theta (*Upper Right*) and gamma (*Lower Right*) illustrate higher theta power and reduced gamma power during arena exploration. We used the gamma histogram intersection, corresponding in this case to the line at a gamma power value of 2.6, as a threshold for detecting transitions between arena- and home-cage–associated brain states. We wanted to assess whether there might be evidence for multiple substates within arena or home-cage conditions to see whether these states appear largely homogeneous or instead are comprised of different components. We thus used the Hartigan dip test, which assesses whether there is sufficient statistical evidence for multiple peaks within a dataset (2). For the dataset analyzed in Fig. S3, we found no evidence for multimodality in either the home cage or the arena for the theta ($P = 0.98$; $P = 0.97$ respectively) and gamma ($P = 0.90$; $P = 0.97$) bands. These results were confirmed (at

$P > 0.1$) in a total of six animals, in total yielding no evidence for multimodality in either behavioral state or frequency band.

SI Analysis of Excursions to DMN Brain State During Arena Exploration

To analyze fluctuations of gamma power within the arena-exploration dataset, we first convolved the gamma power time course with a boxcar ($l = 3$) for some temporal smoothing. In Fig. S4, we plot this time course corresponding to about 20 min of arena exploration for a representative dataset, along with the horizontal line that separates arena from home-cage distributions (Fig. S3). It is evident that for most of the time period the gamma power remains below the threshold line, consistent with the robust gamma suppression observed in the arena. However, five threshold crossings are evident, during which the gamma power exceeds the threshold value and thus enters into a region that is normally characteristic of the default brain state. To visualize these trajectories in theta–gamma state space, we plotted the peak value above threshold (white symbol) and a history of the previous 20 s (black symbols) for each of the five threshold crossings. Note that the theta–gamma values shown correspond to the original (non-smoothed) data. The duration of each threshold crossing is shown above each panel. Based on this sample dataset, we note that gamma suppression was prevalent during arena exploration, and excursions into a high-gamma default mode-like state occurred rarely, around once every 4 min. The duration of these excursions tended to be short and did not exceed 30 s. During the excursions, the gamma values did not attain levels as high as those that occurred in the home cage but remained rather near the values characteristic of the arena. There was no particular trend in terms of theta activity before gamma threshold crossings, which were preceded by increasing, decreasing, or unchanged theta values.

To corroborate these effects observed in the sample session, we performed these analyses in six rats. Each dataset consisted, as above, of about 20 min of BF data in the arena and home cage. The results, shown in Fig. S5, are quite similar to the findings for the sample dataset in Fig. S4. We found on average eight excursions during the 20 min spent in the arena, corresponding to about one excursion every 2–3 min. Excursions lasted between 8 and 44 s, with an average duration of 16 ± 8 s. Based on a comparison of LFP power at the gamma peak to the average values 4–8 s before the peak, gamma transitions were associated with clear increases in gamma power (0.56 ± 0.27, paired t tests: $P \ll 0.001$), but no concomitant significant modulations in theta power (-0.01 ± 0.82, paired t tests: $P > 0.1$) were found.

SI Locomotion During Arena and Object Exploration

In this study, we document gamma LFP suppression in the BF during both empty arena exploration and exploration of objects placed inside this arena. In both behavioral conditions, rats tended to visit the entire arena, as documented in Fig. 2. We therefore expected locomotion to be generally similar in the two behavioral contexts, with the exception that rats are likely to be stationary during object exploration, and thus we anticipated more stationary behavior in this case. This pattern of results corresponds exactly to our measurements ($n = 4$ rats) using video-tracking analysis of the geometrical center of the animals, as shown in the histogram of movement speed values in Fig. S6. We found that quasi-stationary behavior (0–2 cm/s) was seen significantly more frequently in the object-exploration than in the arena-exploration condition (paired t test; $P < 0.05$), an effect reflected by slightly more frequent occupancy of higher

movement-speed bins (upwards of about 5 cm/s) in the arena-exploration condition.

SI Simultaneous LFP Spectrograms for the BF and ACC

To illustrate the close link that we have documented between gamma activations in the BF and ACC, we show here an example of a dataset from two rats comparing simultaneous recordings in these two structures in the home cage and the arena. As documented using statistical tests, i.e., coherence analysis and Granger causality, in Fig. 6 of the main text, these single-session examples illustrate that gamma fluctuations in the BF and ACC were highly coherent, providing further support for the notion that these two structures cooperate to maintain the default brain state.

SI Materials and Methods

Animals and Stereotactic Surgery. Adult male Long Evans rats (80–120 d old) were used in this study. Rats were maintained under a constant 12/12-h light/dark cycle with access to food and water ad libitum. For surgeries, animals were anesthetized with ketamine (100 mg/kg) and xylazine (20 mg/kg), and anesthesia was maintained using isoflurane (around 2%) in pure O_2 inhalation. We used tungsten microelectrodes (FHC), 200 μm in diameter, with 150-kΩ impedance for implantation in the BF [anterior/posterior (AP) −0.8 mm, mediolateral (ML) 2.8 mm, dorsoventral (DV) −8.2 mm from bregma], V1 (AP 1 mm, ML 3.5 mm, DV −1 mm from lambda), and ACC (AP 3.5 mm, ML 0.8 mm, DV −3.0 mm from bregma). Stainless-steel screws above the cerebellum served as the reference and ground for electrodes. For bipolar recordings, two tungsten electrodes were attached with dental cement flush on the vertical axis and with a horizontal tip separation of 200 μm. The connector and leads were fixed to the animal's skull and stabilized with dental cement.

Data Acquisition. Connectors on the head were attached to the miniature data logger (Neurologger 2A), with four channels for LFP recording and an on-board 3D accelerometer for monitoring movement. LFPs were digitized at 1.6 kHz. An infrared receiver on the neurologger was used to mark events such as arena/home cage transitions. LFPs were continuously recorded in all experimental conditions. For tethered recordings (BioAmp Processor; Tucker-Davis Technology), we acquired LFPs and single units at a sampling rate of 1.6 kHz and 24 kHz, respectively.

Arena and Object Exploration. Our testing apparatus was composed of a rectangular arena (70 × 70 × 45 cm) with a camera mounted 100 cm above the arena floor, as described previously (3). Arena and home-cage recordings took place in the same room. The arena-exploration task consisted of two 10-min trials/d (10 min) for a total of 3 d, with an intertrial interval of 45 min, during which time the animal was returned to its home cage. On day 4 the rat explored the arena in the presence of two identical novel objects. We used ELAN behavioral tracking software (https://tla.mpi.nl/tools/tla-tools/elan/; Max Planck Institute for Psycholinguistics) (4) for frame-by-frame analysis of rat behavior. Object exploration was defined as the time during which the animal's nose was <1 cm from the object.

Preprocessing and Spectral Analysis. LFPs were down-sampled to 400 Hz and were partitioned into 2- or 10-s epochs for further analysis. Epochs containing artifacts were rejected by generating a histogram of peak-to-peak amplitude for each epoch and rejecting epochs during which this value exceeded the median plus 1 SD; generally, 1–4% of the epochs were rejected using this criterion. Artifact-free LFPs were used for all further analyses.

Power spectra were calculated for each epoch by fast Fourier transform. Gamma power was calculated by taking the mean value of the power spectrum between 30 and 80 Hz. Spectrograms were calculated using multitaper spectral analysis (5). For analysis of the relationship between gamma power and movement, accelerometer data were split into four quartiles, and the corresponding mean gamma power of each quartile was quantified and averaged across animals.

Phase-Locking Analysis. Single units were first sorted from the continuously recorded data, sampled at 24 KHz, and bandpass filtered between 100 Hz and 8 KHz, using Wav_clus (github.com/csn-le/wave_clus) (6). LFP data were initially bandpass filtered between 30 and 80 Hz, and phase angles were extracted from the Hilbert-transformed data. Spiking activity was then binned into 25 14.4° bins, and units were considered to be phase locked if they showed a nonuniform distribution across bins [Hodges–Ajne test (7)]; otherwise they were considered to be not phase locked. The raw LFP data were then bandpass filtered at 10 10-Hz-wide bands, 1–10, 10–20 . . . 90–100, and the process was repeated for our phase-locked units. A PLI was calculated for each band pass as the coefficient of variation of the probability scores across the phase angles.

Coherence Spectral Analyses. We performed coherence spectral analyses between BF and cortical regions using the BSMART toolbox (8) as in our previous study (1), based on recordings from four animals. After data normalizing and detrending, we fitted an autoregressive model to time series of 2-s epochs with a model order number of 15. Based on autoregressive-modeled data, bivariate coherence spectral analyses were computed across conditions and pairs of recording sites. For statistical comparison across conditions and recording pairs, repeated-measures ANOVAs (SPSS) were conducted based on the area under the curve of the gamma frequency range between 40 and 60 Hz.

Granger Causality Analyses During BF Gamma Bursts. To study directional influences in the gamma band in the BF, ACC, and VC, Granger causality spectral analyses were performed during BF gamma burst epochs. BF gamma bursts were detected by detrending and bandpass filtering (40–60 Hz) the LFP signal. The amplitude threshold was calculated individually for each animal and session as 2.5 SDs from the mean. Burst beginning and end times were then defined as the points at which the amplitude fell below 1.5 SDs before and after the detected burst. Only gamma bursts with a length of 100–800 ms were included in subsequent segmentation. Unfiltered LFP signals were segmented into epochs of 160 ms centered on the detected bursts. Based on those epochs, we performed bivariate ($n = 7$ animals) and trivariate ($n = 4$ animals) Granger causality analyses by using the MVGC multivariate Granger causality toolbox (9). Here, the LFP epochs were transformed to auto-covariance data by setting the maximal model order of 15 according to the Akaike Information Criterion. Subsequently, pairwise Granger causality spectra analyses were performed, and we conducted a statistical comparison averaged across pairs of recording sites in the gamma frequency range (40–60 Hz) using paired t tests and repeated-measures ANOVAs (SPSS).

Histological Verification of Electrode Targets. Electrode sites were electro-coagulated with a constant current for 20 s. After perfusion, fixed brain tissue was cut into 60-μm-thick coronal sections and stained with cresyl violet. The anatomical location of each electrode was determined from the coagulation mark using a rat brain atlas (10).

1. Nair J, et al. (2016) Gamma band directional interactions between basal forebrain and visual cortex during wake and sleep states. *J Physiol Paris* 110:19–28.
2. Hartigan JA, Hartigan PM (1985) The dip test of unimodality. *Ann Stat* 13:70–84.
3. Nair J, Topka M, Khani A, Isenschmid M, Rainer G (2014) Tree shrews (Tupaia belangeri) exhibit novelty preference in the novel location memory task with 24-h retention periods. *Front Psychol* 5:303.

4. Lausberg H, Sloetjes H (2009) Coding gestural behavior with the NEUROGES–ELAN system. *Behav Res Methods* 41:841–849.
5. Bokil H, Andrews P, Kulkarni JE, Mehta S, Mitra PP (2010) Chronux: A platform for analyzing neural signals. *J Neurosci Methods* 192:146–151.
6. Quiroga RQ, Nadasdy Z, Ben-Shaul Y (2004) Unsupervised spike detection and sorting with wavelets and superparamagnetic clustering. *Neural Comput* 16:1661–1687.
7. Berens P (2009) CircStat: A MATLAB toolbox for circular statistics. *J Stat Softw* 31:1–21.
8. Cui J, Xu L, Bressler SL, Ding M, Liang H (2008) BSMART: A Matlab/C toolbox for analysis of multichannel neural time series. *Neural Netw* 21:1094–1104.
9. Barnett L, Seth AK (2014) The MVGC multivariate granger causality toolbox: A new approach to granger-causal inference. *J Neurosci Methods* 223:50–68.
10. Paxinos G, Watson C (1986) *The Rat Brain in Stereotaxic Coordinates* (Academic, Sydney), 2nd Ed.
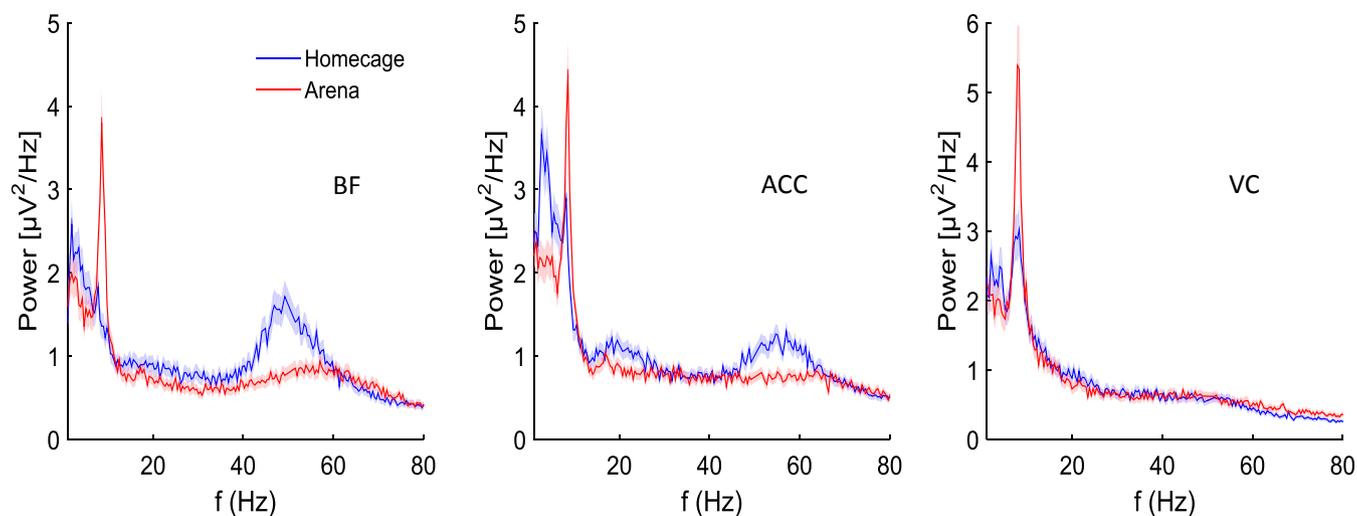
Fig. S1. Wide-band LFP spectra for a sample single animal. The plots show mean ± SEM. f, frequency.
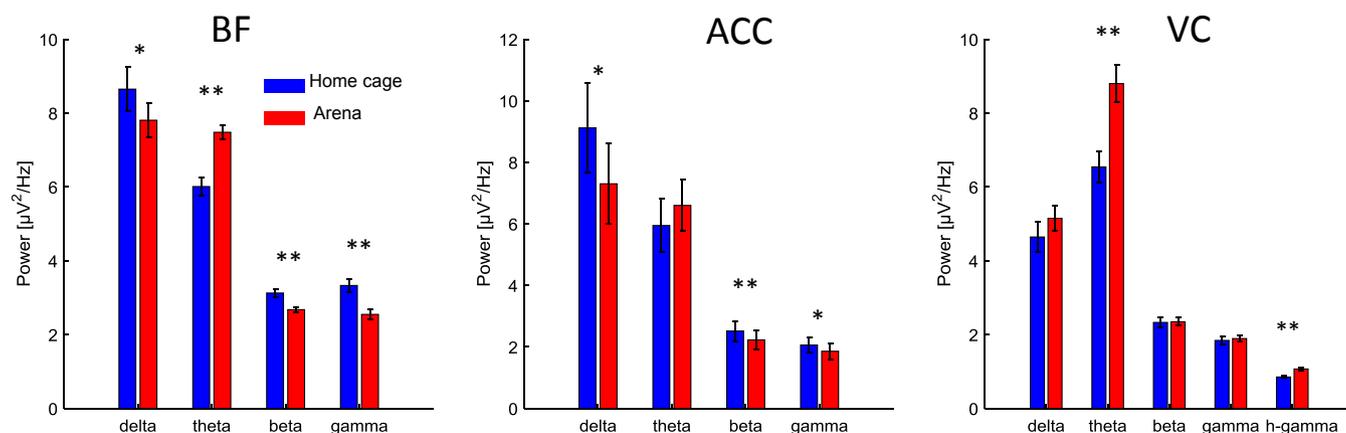
Fig. S2. Group analysis of wide-band LFP spectra. Bar charts illustrate power modulations for distinct frequency bands: blue, home cage; red, arena. *$P < 0.05$, **$P < 0.001$, paired t test.

Fig. S3. BF LFP state diagram. (*Left*) Scatter plot illustrating the distribution of gamma vs. theta LFP power in a sample dataset. (*Right*) Histograms of theta power (*Upper*) and gamma power (*Lower*) demonstrating the systematic effect of behavioral condition on both parameters: blue, home cage; red, arena.

Fig. S4. BF gamma-band LFP excursions to the default brain state during arena exploration. (*Upper*) Running average of gamma power during a sample 10-min recording. Threshold (dotted line) crossings identify excursions into high-gamma activations during exploration. (*Lower*) Trajectories for the five identified default brain state excursions, showing the history of gamma–theta activations before the identified gamma peak (dark symbols) and the activation at the peak (white symbol).

Fig. S5. Group analysis of BF gamma-band LFP excursions to the default brain state during arena exploration. Each panel illustrates all the gamma-band LFP excursions that occurred in the analyzed arena-exploration session in each of the six animals analyzed. White markers delineate endpoints of excursions, and dark symbols show the history of activity before excursion peak.

Fig. S6. Analysis of locomotion during arena and object exploration using video analysis. Histograms show observed locomotion speeds during empty arena-exploration and object-exploration sessions. Asterisk denotes statistical significance ($P < 0.05$).

Fig. S7. Examples of single-session spectrograms for the BF (*Upper*) and ACC (*Lower*) in two different animals (*Left* and *Right*). Arena exploration occurred at $t < 0$, and animals were transferred to the home cage at $t = 0$, so that times $t > 0$ correspond to the home-cage behavioral condition.